Electronic Supplementary Material

Advancing Nonlinear Optics: Discovery and Characterization of New Non-Centrosymmetric Phenazine-Based Halides

Yibo Cui,[a] Jindong Cao,[a] Jiawei Lin,[b] Chunxiao Li,[c] Jiyong Yao,[c] Kunjie Liu,[a] An Hou,[a] Zhongnan Guo,[b] Jing Zhao,*[a] Quanlin Liu*[a]

[a.] The Beijing Municipal Key Laboratory of New Energy Materials and Technologies,
School of Materials Science and Engineering, University of Science and Technology Beijing, Beijing 100083, P. R. China
Jing Zhao, E-mail: jingzhao@ustb.edu.cn. Quanlin Liu, E-mail: qlliu@ustb.edu.cn.

[b.] The Beijing Municipal Key Laboratory of New Energy Materials and Technologies, School of Materials Sciences and Engineering and Chemistry and Biological Engineering, University of Science and Technology Beijing, Beijing 100083, China.

[c.] Center for Crystal Research and Development, Key Laboratory of Functional Crystals and Laser Technology, Technical Institute of Physics and Chemistry, Chinese Academy of Sciences, Beijing 100190, China.

SUPPORTING INFORMATION

CONTENTS

1. Figures

2. Tables

1. Figures

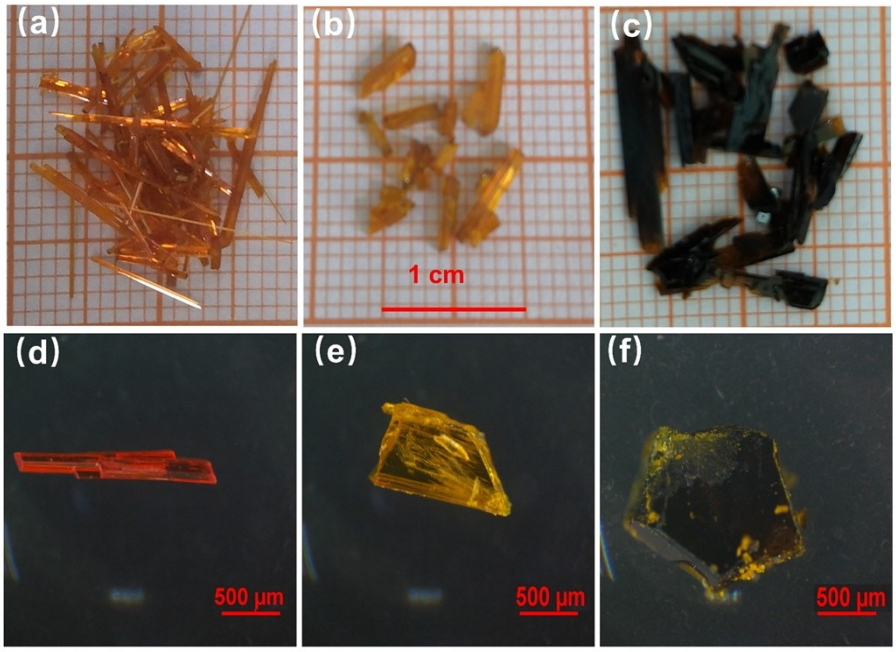

Figure S1. Photographs of $(C_{12}H_9N_2)PbCl_3$ (a), $(C_{12}H_9N_2)SbCl_4$ (b), and $(C_{12}H_9N_2)_2InBr_4 \cdot Br$ (c). Fluorescence photographs of $(C_{12}H_9N_2)PbCl_3$ (d), $(C_{12}H_9N_2)SbCl_4$ (e), and $(C_{12}H_9N_2)_2InBr_4 \cdot Br$ (f).

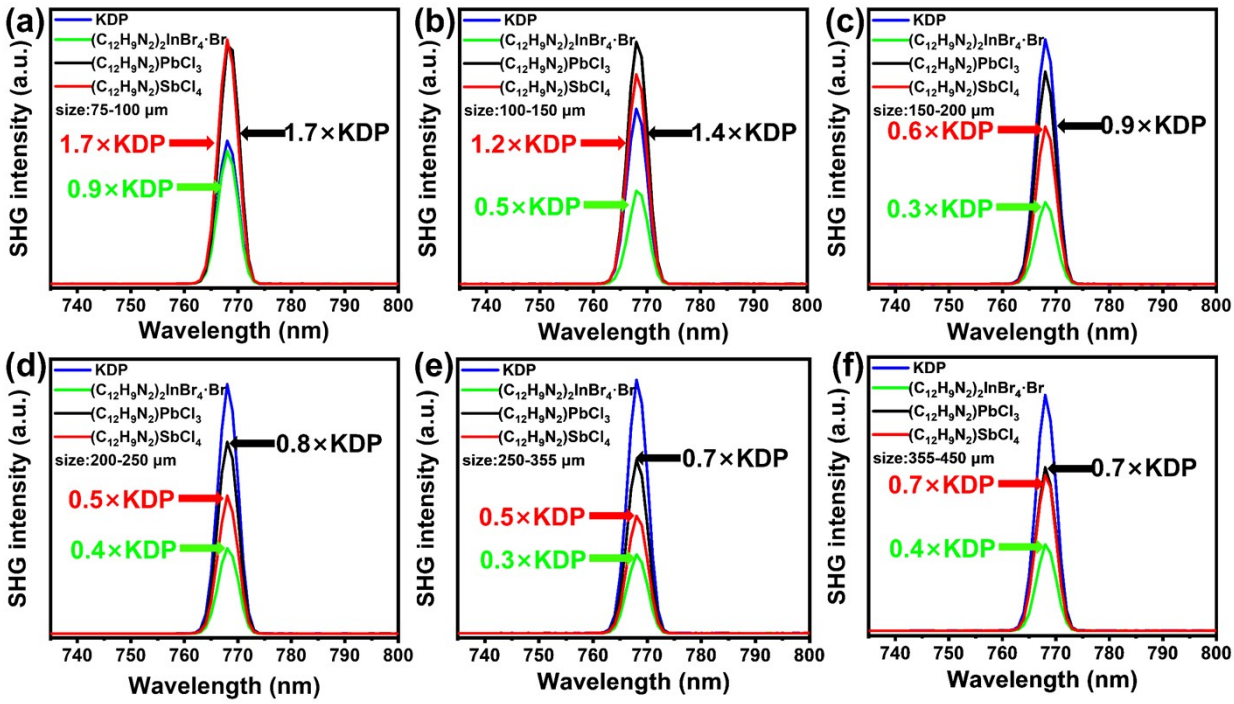

Figure S2. Nonlinear optical responses and intensity ratios to KDP for $(C_{12}H_9N_2)PbCl_3$, $(C_{12}H_9N_2)SbCl_4$, and $(C_{12}H_9N_2)_2InBr_4{\cdot}Br$ at different particles.

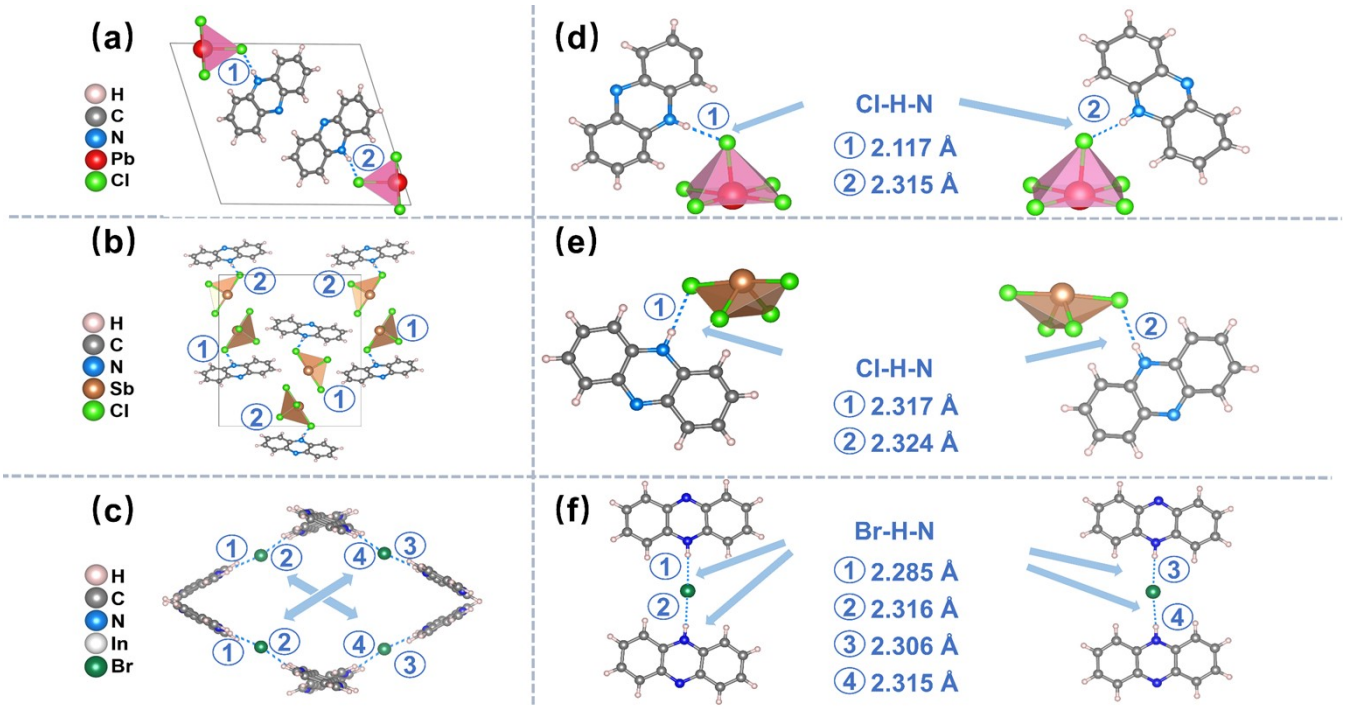

Figure S3. Spatial H-bond distributions for $(C_{12}H_9N_2)PbCl_3$ (a), $(C_{12}H_9N_2)SbCl_4$ (b), $(C_{12}H_9N_2)_2InBr_4{\cdot}Br$ (c), and their specific connections in two environments (d, e and f).

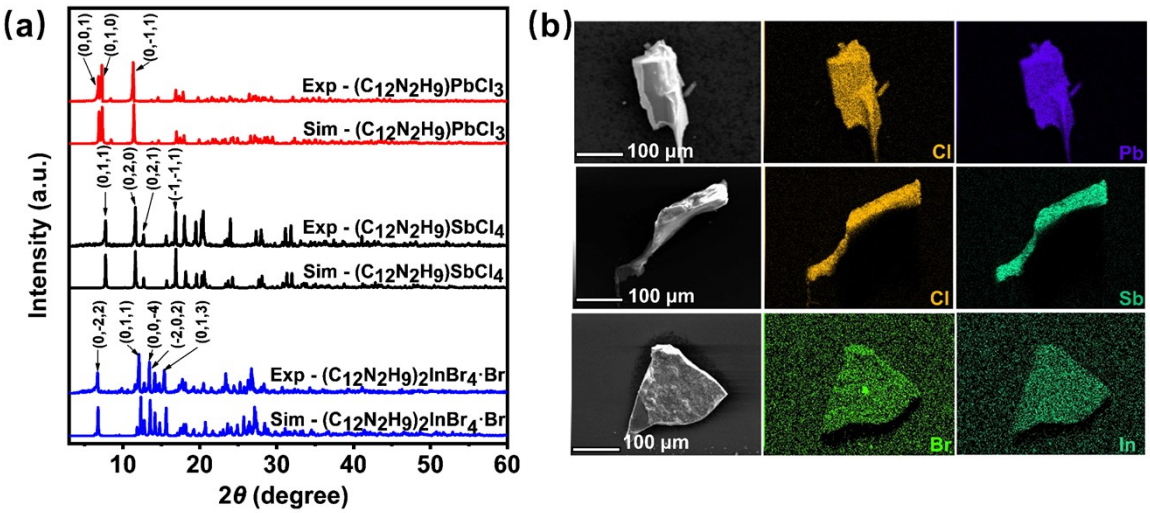

Figure S4. (a) PXRD patterns of the three compounds. (b) EDS mapping demonstrates the homogenous distribution of elements in the examined compounds.

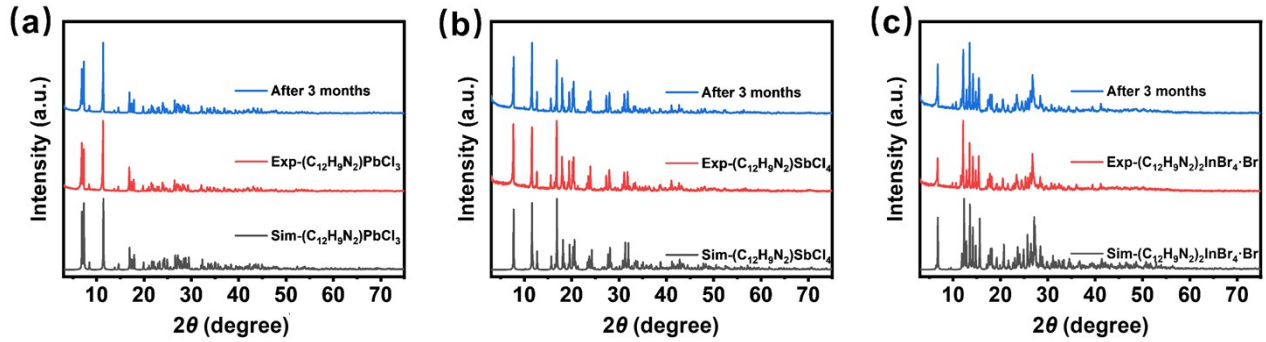

Figure S5. PXRD comparison of $(C_{12}H_9N_2)PbCl_3$ (a), $(C_{12}H_9N_2)SbCl_4$ (b), and $(C_{12}H_9N_2)_2InBr_4{\cdot}Br$ (c) before and after three months.

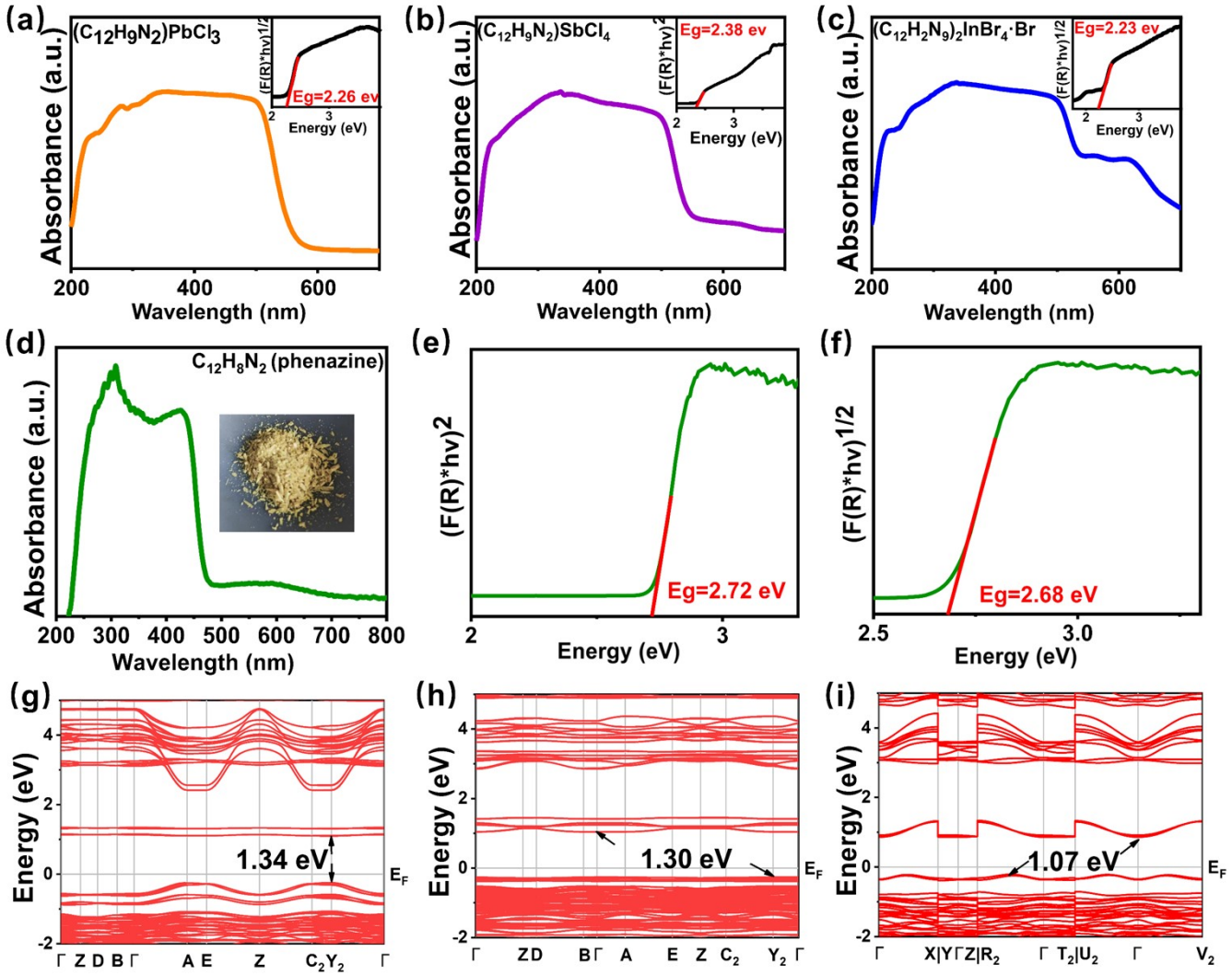

Figure S6. The UV-Visible absorption spectra and experimental band gaps are provided for $(C_{12}H_9N_2)PbCl_3$ (a), $(C_{12}H_9N_2)SbCl_4$ (b), and $(C_{12}H_9N_2)_2InBr_4{\cdot}Br$ (c). UV-Vis absorption spectrum of $C_{12}H_8N_2$, with photograph inset (d), direct optical bandgap of $C_{12}H_8N_2$ (e), indirect optical bandgap of $C_{12}H_8N_2$ (f). Additionally, the theoretically calculated band gap diagrams are shown for $(C_{12}H_9N_2)PbCl_3$ (g), $(C_{12}H_9N_2)SbCl_4$ (h), and $(C_{12}H_9N_2)_2InBr_4{\cdot}Br$ (i).

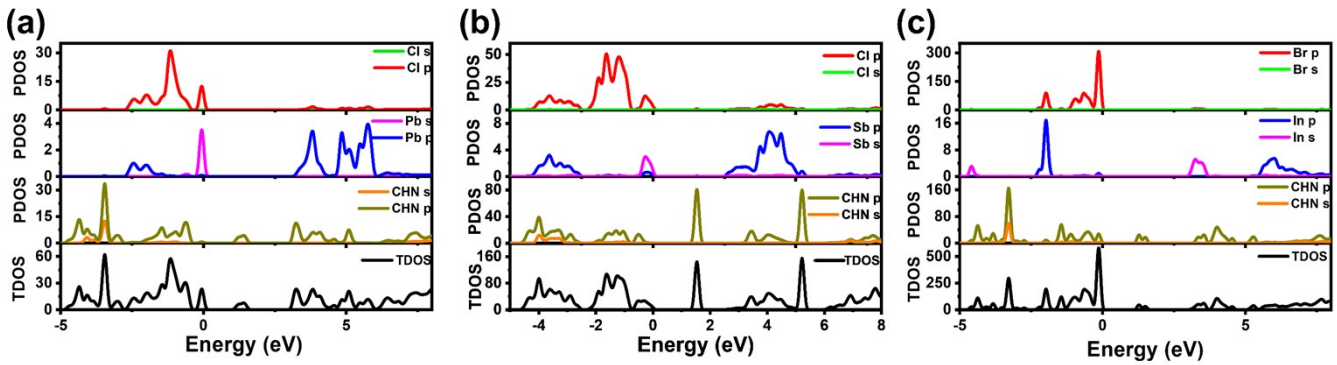

Figure S7. The PDOS and TDOS diagrams of $(C_{12}H_9N_2)PbCl_3$ (a), $(C_{12}H_9N_2)SbCl_4$ (b), and $(C_{12}H_9N_2)_2InBr_4{\cdot}Br$ (c).

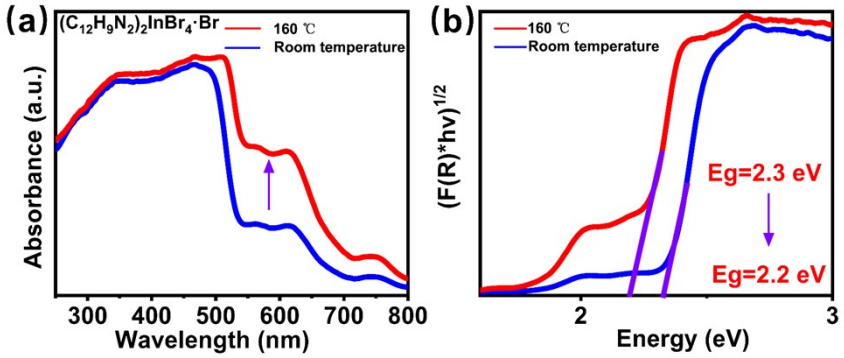

Figure S8. UV-Vis absorption spectra of $(C_{12}H_9N_2)_2InBr_4{\cdot}Br$ at room temperature and 160 °C (a), and their corresponding bandgaps (b).

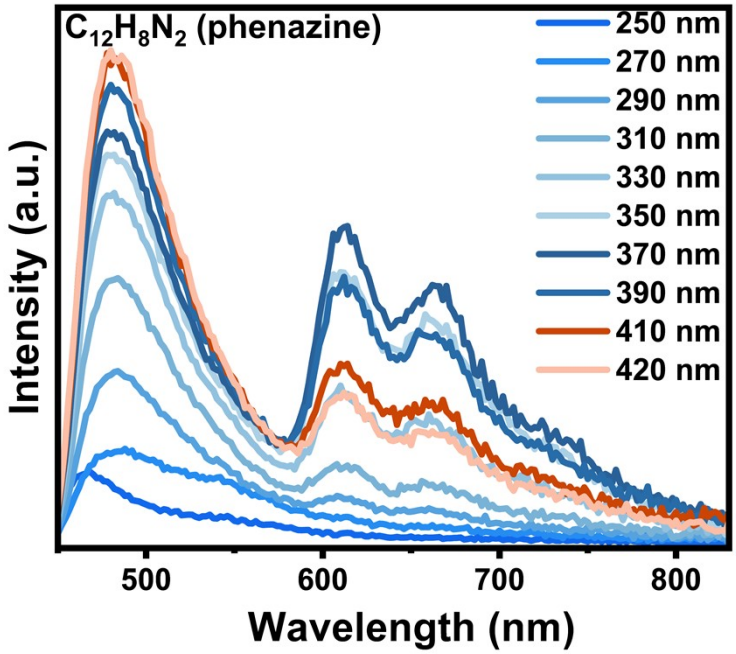

Figure S9. The emission spectrum of the organic compound $C_{12}H_8N_2$ at various excitation wavelengths.

2.Table

Table S1. Atomic coordinates (×10^4) and equivalent isotropic displacement parameters (Å^{2}x10^3) for $(C_{12}H_9N_2)PbCl_3$ at 150.0 K with estimated standard deviations in parentheses.

Label	*x*	*y*	*z*	Occupancy	U_{eq}^*
Pb(1)	-10011(1)	-8601(1)	-9655(1)	1	29(1)
Pb(2)	-13833(1)	-10343(1)	-11643(1)	1	28(1)
Cl(2)	-5640(20)	-7003(7)	-10018(7)	1	53(2)
Cl(5)	-9130(20)	-8620(7)	-11989(7)	1	56(2)
N(2)	-5960(60)	-4150(20)	-14620(20)	1	35(5)
C(7)	-8720(60)	-5390(20)	-13090(20)	1	41(6)
N(1)	-9610(40)	-2332(17)	-14005(17)	1	28(4)
C(3)	-9830(60)	-3330(20)	-13320(20)	1	28(5)
C(2)	-7150(50)	-2130(20)	-14957(19)	1	33(6)
C(4)	-11910(60)	-3560(20)	-12534(18)	1	30(6)
C(5)	-12210(60)	-4610(20)	-11951(15)	1	37(7)
C(12)	-5210(60)	-922(18)	-16460(20)	1	25(4)
C(1)	-7220(50)	-1087(17)	-15553(16)	1	18(3)
C(9)	-5770(60)	-3010(20)	-15160(20)	1	28(5)
C(10)	-3430(60)	-2920(20)	-16070(20)	1	41(7)
C(11)	-3390(70)	-1720(20)	-16730(20)	1	37(6)
C(6)	-10700(70)	-5480(20)	-12160(20)	1	34(5)
N(3)	-7930(50)	-4867(17)	-16815(17)	1	21(4)
C(16)	-10360(50)	-6110(20)	-15260(20)	1	28(5)
C(15)	-8450(60)	-5820(20)	-16190(20)	1	26(5)
C(13)	-5570(60)	-3590(20)	-18238(17)	1	24(4)
C(14)	-6080(60)	-4690(16)	-17553(19)	1	20(4)
C(24)	-3310(70)	-3370(20)	-19010(20)	1	30(5)
C(22)	-1960(50)	-5380(20)	-18840(20)	1	41(7)
N(4)	-4840(40)	-6604(16)	-17262(16)	1	22(4)
Cl(1)	-10306(17)	-8603(6)	-7628(6)	1	33(2)
Cl(4)	-13575(19)	-10348(6)	-13663(6)	1	36(2)
Cl(6)	-18274(14)	-11966(4)	-11288(4)	1	24(2)
Cl(3)	-14665(12)	-10289(4)	-9332(4)	1	22(2)
C(8)	-8210(60)	-4310(20)	-13650(20)	1	33(6)
C(21)	-4210(60)	-5517(19)	-17839(18)	1	23(4)
C(19)	-7110(60)	-7930(20)	-15760(20)	1	42(6)
C(23)	-1450(60)	-4298(19)	-19377(19)	1	38(6)
C(18)	-9030(60)	-8060(20)	-14900(20)	1	38(6)
C(17)	-10730(60)	-7048(19)	-14689(17)	1	23(4)

C(20)	-6390(50)	-6797(13)	-16476(18)	1	21(4)

*U_{eq} is defined as one third of the trace of the orthogonalized U_{ij} tensor.

Table S2. Atomic coordinates (x10^4) and equivalent isotropic displacement parameters (Å^{2}x10^3) for $(C_{12}H_9N_2)SbCl_4$ at 293(2) K with estimated standard deviations in parentheses.

Label	*x*	*y*	*z*	Occupancy	U_{eq}*
Sb(1)	10545(2)	6298(1)	3676(1)	1	30(1)
Sb(2)	-552(2)	5615(1)	1321(1)	1	30(1)
Cl(7)	-1248(7)	4295(4)	610(2)	1	54(2)
Cl(6)	3587(6)	5478(4)	1417(3)	1	56(2)
Cl(5)	-461(8)	4740(4)	2560(2)	1	55(2)
N(4)	3810(20)	5804(10)	9083(7)	1	37(3)
N(1)	6250(20)	6054(9)	5972(7)	1	32(3)
C(7)	4490(30)	8676(15)	6225(10)	1	66(5)
C(22)	6850(30)	6213(15)	8312(9)	1	43(5)
N(3)	7470(20)	5406(11)	8234(7)	1	44(4)
C(15)	3010(30)	4318(14)	9274(9)	1	46(4)
C(14)	3620(30)	3456(11)	9186(9)	1	52(4)
C(9)	6980(30)	7604(14)	5694(9)	1	45(5)
C(5)	3890(30)	7131(11)	6442(9)	1	36(4)
C(11)	5080(30)	5405(12)	6241(8)	1	31(4)
C(6)	3230(30)	8063(14)	6495(9)	1	51(5)
C(10)	5730(30)	6943(13)	5995(9)	1	36(4)
C(17)	4980(30)	6465(12)	8734(9)	1	37(4)
C(18)	4320(30)	7373(9)	8828(9)	1	39(4)
C(12)	5610(30)	4576(13)	6165(10)	1	51(5)
C(16)	4320(30)	4982(11)	8966(9)	1	32(4)
C(23)	6300(20)	4760(12)	8564(7)	1	32(4)
Cl(1)	10158(8)	5421(4)	4955(2)	1	52(2)
Cl(2)	11300(6)	7634(4)	4398(2)	1	51(2)
Cl(4)	10405(7)	7178(4)	2419(2)	1	59(2)
Cl(3)	6421(7)	6421(5)	3583(3)	1	65(2)
C(3)	1890(20)	5035(11)	7017(7)	1	36(3)
C(2)	2520(30)	4186(16)	6907(11)	1	59(5)
C(1)	4290(30)	3992(15)	6495(11)	1	60(5)
N(2)	2610(20)	6530(9)	6740(6)	1	32(3)
C(4)	3210(20)	5665(12)	6664(7)	1	27(3)
C(21)	8040(20)	6937(13)	8021(9)	1	47(4)
C(24)	6770(30)	3910(13)	8449(10)	1	44(4)

C(19)	5520(30)	8039(13)	8508(10)	1	43(4)
C(13)	5510(30)	3257(12)	8777(8)	1	52(4)
C(8)	6380(30)	8423(15)	5814(10)	1	61(5)
C(20)	7510(30)	7783(14)	8095(9)	1	42(4)
Cl(8)	-260(7)	6488(4)	24(2)	1	48(2)

*U_{eq} is defined as one third of the trace of the orthogonalized U_{ij} tensor.

Table S3. Atomic coordinates (x10^4) and equivalent isotropic displacement parameters (Å^{2}x10^3) for $(C_{12}H_9N_2)_2InBr_4 \cdot Br$ at 150.00 K with estimated standard deviations in parentheses.

Label	*x*	*y*	*z*	Occupancy	U_{eq}*
In(01)	1901(1)	-2162(1)	6630(1)	1	38(1)
In(02)	7148(1)	8054(1)	6682(1)	1	40(1)
Br(03)	2087(1)	-633(2)	4219(1)	1	44(1)
Br(04)	8002(1)	10463(2)	4146(1)	1	45(1)
Br(05)	2085(1)	-1461(2)	5711(1)	1	49(1)
Br(06)	7972(1)	8730(2)	7527(1)	1	47(1)
Br(07)	7712(1)	9934(2)	5971(1)	1	50(1)
Br(08)	7357(1)	4814(2)	6471(1)	1	54(1)
Br(09)	2868(1)	-4886(2)	6855(1)	1	63(1)
Br(0A)	5363(1)	8598(2)	6725(1)	1	62(1)
Br(0B)	2473(1)	250(2)	7229(1)	1	64(1)
Br(0C)	143(1)	-2721(2)	6719(1)	1	64(1)
C(00D)	5947(8)	8283(12)	4898(4)	1	41(2)
N(00E)	10023(5)	12310(10)	4445(3)	1	35(2)
N(00F)	6084(5)	8145(9)	3990(3)	1	34(2)
N(00G)	11763(5)	14043(10)	4661(3)	1	34(2)
N(00H)	61(5)	-2470(9)	3964(3)	1	34(2)
C(00I)	-151(7)	-2807(14)	4864(4)	1	43(2)
N(00J)	-1658(5)	-4235(10)	3724(3)	1	37(2)
N(00K)	5823(5)	3139(9)	4499(3)	1	34(2)
C(00L)	10534(6)	12899(11)	4050(4)	1	32(2)
C(00M)	11967(7)	14400(12)	3763(4)	1	41(2)
C00N()	-459(6)	-3066(12)	4352(4)	1	35(2)
C(00O)	5994(7)	3045(12)	3597(4)	1	39(2)
C(00P)	-1354(6)	-3977(12)	4211(4)	1	35(2)
C(00Q)	4642(8)	1931(14)	3061(4)	1	44(2)
C(00R)	4493(6)	1996(12)	3956(4)	1	34(2)
C(00S)	11659(7)	14105(14)	3277(4)	1	45(2)
N(00T)	4262(6)	6670(10)	3851(3)	1	37(2)
C(00U)	4466(7)	7182(13)	5230(4)	1	43(2)

C(00V)	11008(7)	13026(13)	5943(4)	1	44(2)
C(00W)	4081(7)	6753(13)	4758(4)	1	41(2)
C(00X)	10771(8)	13215(13)	3166(4)	1	45(2)
C(00Y)	5597(8)	2631(13)	3129(5)	1	47(3)
C(00Z)	5392(8)	7948(14)	5303(4)	1	44(2)
N(010)	3987(5)	1712(9)	4380(3)	1	36(2)
C(011)	10209(7)	12626(12)	3539(4)	1	37(2)
C(012)	4630(6)	7083(12)	4323(4)	1	35(2)
C(013)	5571(6)	7842(11)	4407(4)	1	34(2)
C(014)	-839(8)	-3242(14)	2456(5)	1	48(3)
C(015)	11546(7)	13645(12)	5560(4)	1	40(2)
C(016)	-732(8)	-3376(13)	5234(4)	1	46(3)
C(017)	11436(7)	13782(12)	4175(4)	1	37(2)
C(018)	11225(7)	13419(11)	5041(4)	1	36(2)
C(019)	5923(8)	7629(14)	2609(4)	1	45(2)
C(01A)	6308(7)	8064(12)	3085(4)	1	39(2)
C(01B)	-1112(7)	-3603(12)	3356(4)	1	39(2)
C(01C)	4104(7)	1594(13)	3460(4)	1	40(2)
C(01D)	10332(7)	12501(12)	4938(4)	1	35(2)
C(01E)	-1608(7)	-4292(14)	5105(5)	1	46(3)
C(01F)	340(7)	-2008(14)	3070(4)	1	43(2)
C(01G)	-222(7)	-2666(12)	3468(4)	1	39(2)
C(01H)	5439(6)	2755(13)	4032(4)	1	39(2)
C(01I)	10120(8)	12104(14)	5828(4)	1	46(2)
C(01J)	5749(6)	7747(11)	3516(4)	1	33(2)
C(01K)	5685(7)	3154(13)	5412(4)	1	43(2)
C(01L)	32(8)	-2278(15)	2577(5)	1	52(3)
C(01M)	5145(8)	2818(14)	5828(5)	1	48(3)
C01N()	4793(7)	7009(12)	3451(4)	1	37(2)
C(01O)	-1387(7)	-3859(13)	2827(4)	1	43(2)
C(01P)	4973(8)	6941(15)	2540(4)	1	47(3)
C(01Q)	-1913(7)	-4589(12)	4612(4)	1	38(2)
C(01R)	9783(7)	11837(12)	5339(4)	1	41(2)
C(01S)	4342(6)	2084(12)	4860(4)	1	35(2)
C(01T)	3799(7)	1728(13)	5286(4)	1	41(2)
C(01U)	5290(7)	2804(12)	4910(4)	1	35(2)
C(01V)	4197(8)	2123(14)	5755(4)	1	46(2)
C(01W)	4426(7)	6610(13)	2950(4)	1	42(2)

*U_{eq} is defined as one third of the trace of the orthogonalized U_{ij} tensor.

Table S4. Under 2090 nm laser irradiation, the SHG intensity of $(C_{12}H_9N_2)PbCl_3$,$(C_{12}H_9N_2)SbCl_4$, and $(C_{12}H_9N_2)_2InBr_4{\cdot}Br$ was compared with that of $AgGaS_2$ at different particle sizes.

Particle size	$(C_{12}H_9N_2)PbCl_3/AgGaS_2$	$(C_{12}H_9N_2)SbCl_4/AgGaS_2$	$(C_{12}H_9N_2)_2InBr_4{\cdot}Br/AgGaS_2$
75-100 μm	0.013	0.014	0.017
100-150 μm	0.015	0.018	0.030
150-200 μm	0.008	0.011	0.013
200-250 μm	0.043	0.015	0.015
250-355 μm	0.018	0.006	0.008
355-450 μm	0.032	0.012	0.009

Table S5. The Olex2 crystal structure refinement parameters for $(C_{12}H_9N_2)PbCl_3$ were compared in two space groups, *P*1 and *P*.

Space group	*P*1	*P*
R_1	2.11%	1.88%
wR_2	4.86%	5.84%
d_{min}(Mo)	0.79	0.79
I/σ	32.7	50.5
R_{int}	3.26%	3.50%
complete	99%	100%
Shift	-0.001	0.000
Max peak	0.5	0.6
Min peak	-1.1	-1.1
GooF	1.055	1.211

Table S6. The Olex2 crystal structure refinement parameters for $(C_{12}H_9N_2)SbCl_4$ were compared in two space groups, $P2_1/c$ and $P2_1$.

Space group	$P2_1$	$P2_1/c$
R_1	2.78%	3.87%
wR_2	6.02%	8.47%
d_{min}(Mo)	0.72	0.72
I/σ	20.1	15.3
R_{int}	6.73%	5.96%
complete	100%	99%
Shift	0.001	0.000
Max peak	0.5	0.6
Min peak	-0.7	-1.0
GooF	1.136	1.011

Table S7. The comparison of the unit cell parameters of $(C_{12}H_9N_2)_2InBr_4 \cdot Br$ at high and low temperatures.

Empirical formula	$(C_{12}H_9N_2)_2InBr_4 \cdot Br$	
Temperature	433.00 K	150.00 K
Crystal system	Monoclinic	Monoclinic
Unit cell dimensions	*a* = 13.72 Å	*a* = 13.86 Å
	b = 7.74 Å	*b* = 7.76 Å
	c = 26.43 Å	*c* = 26.18 Å
	α = 90°	*α* = 90°
	β = 90°	*β= 90°*
	γ = 90°	*γ* = 90°
Volume	2805 Å^3	2704 Å^3